

The dust content of the most metal-poor star-forming galaxies

Raffaella Schneider¹*, Leslie Hunt² and Rosa Valiante¹

¹INAF/Osservatorio Astronomico di Roma, Via di Frascati 33, 00040 Monte Porzio Catone, Italy

²INAF/Osservatorio Astrofisico di Arcetri, Largo Enrico Fermi 5, 50125 Firenze, Italy

draft version 20 November 2015

ABSTRACT

Although dust content is usually assumed to depend uniquely on metallicity, recent observations of two extremely metal-poor dwarf galaxies have suggested that this may not always be true. At a similar oxygen abundance of $\sim 3\% Z_{\odot}$, the dust-to-gas and dust-to-stellar mass ratios in SBS 0335–052 and IZw 18 differ by a factor 40–70 according to including molecular gas or excluding it. Here we investigate a possible reason for this dramatic difference through models based on a semi-analytical formulation of chemical evolution including dust. Results suggest that the greater dust mass in SBS 0335–052 is due to the more efficient grain growth allowed by the high density in the cold interstellar medium (ISM), observationally inferred to be almost 20 times higher than in IZw 18. Our models are able to explain the difference in dust masses, suggesting that efficient dust formation and dust content in galaxies, including those with the highest measured redshifts, depend sensitively on the ISM density, rather than only on metallicity.

Key words: ISM: abundances — ISM: evolution — galaxies: starburst — galaxies: dwarf — galaxies: evolution — galaxies: individual: SBS0335-052 — galaxies: individual: IZw18

1 INTRODUCTION

The dust content in galaxies is intimately linked to their evolutionary history. Nevertheless, the mass of the dust in the interstellar medium (ISM), and its ratio with the gas mass (dust-to-gas ratio, DGR), are critical parameters for establishing the evolutionary state of a galaxy. However, the complex interplay between dust destruction and dust formation mechanisms (e.g., Dwek 1998; Bianchi & Schneider 2007; Jones & Nuth 2011), makes it difficult to infer evolutionary trends from dust alone.

Another signature of evolutionary status is a galaxy’s metal abundance, generally quantified by the nebular abundance of oxygen, O/H. Although dust grains consist mainly of metals, grains are not the dominant contributor to the metal budget of galaxies (Peeples et al. 2014). Nevertheless, the metals in dust and the metals in gas are expected to be coupled through the ISM energy cycle, and much work has been focused on comparing dust content with metallicity. Indeed, the DGR and O/H seem to be fairly well correlated both in the Milky Way and in nearby star-forming galaxies. Observations of the DGR compared with the gas-phase metallicity suggest approximate linearity between the two (e.g., Issa et al. 1990; Schmidt & Boller 1993; Draine et al. 2007), a trend which is generally true even for gradients of the DGR within galaxies, which tend to follow the radial changes in metallicity (e.g., Muñoz-Mateos et al. 2009; Magrini et al. 2011). Since the seminal work by Dwek (1998), many galaxy evolution models and models of the ISM now *assume* that dust content is proportional to metallicity

(e.g., Granato et al. 2000; Wolfire et al. 2003; Gnedin et al. 2009; Krumholz et al. 2009b). In the ISM models, this assumption is directly related to the capability of the gas to self-shield from intense ultraviolet radiation, and is thus crucial for the formation of H_2 .

However, new results with *Herschel* and ALMA challenge the assumption of a direct (linear) correspondence of the DGR with metal abundance. Based on dust masses calculated with *Herschel* data from the Dwarf Galaxy Survey (Madden et al. 2013), Rémy-Ruyer et al. (2014) found that the DGR is linearly proportional to O/H only to $12+\log(O/H)\sim 8$ ($20\% Z_{\odot}$); at lower metallicities the dependence of DGR is steeper, implying relatively less dust (or more gas) at lower abundances. By including new ALMA data at $870\ \mu\text{m}$, Hunt et al. (2014, hereafter H14) derive vastly different DGRs even at the same metallicity, in particular for the two most metal-poor star-forming galaxies in the Local Universe, SBS 0335–052 and IZw 18, both at $\sim 3\% Z_{\odot}$. As shown in Fig. 1 (adapted from Hunt et al. 2014, see also Sects. 2.1 – 2.3) the DGRs of these two galaxies differ by almost two orders of magnitude, despite their similar metallicity.

In this paper, we examine possible reasons for this dramatic difference in dust content at similar metallicity in these two galaxies. We first discuss their basic properties in Sect. 2. Then, in Sect. 3, we explore the origin of the observed dust in SBS 0335–052 and IZw 18 using a semi-analytic chemical evolution model with dust. The model has been first introduced by Valiante et al. (2009) and then applied by Valiante et al. (2011, 2012, 2014) and de Bressan et al. (2014) within the context of a hierarchical model for the evolution of cosmic structures, as predicted by the concordance Λ CDM model. Here we do not investigate the hierarchical evolu-

* E-mail: raffaella.schneider@oa-roma.inaf.it

tion of SBS 0335–052 and IZw 18, but rather limit the discussion to their chemical evolution assuming that they evolve in isolation with a constant star formation rate (SFR)¹. Below, we only briefly describe the model, referring interested readers to the above papers for a more detailed description. We discuss implications of our results for high-redshift dust formation in star-forming galaxies in Sect. 4, and our conclusions are given in Sect. 5.

2 OBSERVED PROPERTIES OF IZw 18 AND SBS 0335–052

The observed properties of the two metal-poor dwarf galaxies that we have adopted for our analysis are presented in Table 1. The observational data and the methods used to infer the physical properties listed in the table have been thoroughly described in H14 and references therein (see in particular Tables 1 and 3 in H14). H14 analyzed dust and gas surface densities and did not include ionized gas. Here we revise the estimates of gas masses in both galaxies relative to H14 in order to take into account the ionized gas component and the spatial extent of cool dust emission. The values obtained for the individual ISM components and the total gas masses are given in Table 1 and shown graphically in Fig. 1.

2.1 Atomic gas masses

Both IZw 18 and SBS 0335–052 are embedded in vast H I envelopes which include other galaxies or galaxy components. SBS 0335–052 has a western component SBS 0335–052W at a distance of ~ 22 kpc within a 64 kpc H I cloud (Pustilnik et al. 2001; Ekta et al. 2009); IZw 18 (main body) lies about 2 kpc away from the “C” component, or Zwicky’s flare, within a diffuse H I cloud extending over ~ 19 kpc (van Zee et al. 1998; Lelli et al. 2012). Thus it is difficult to determine exactly where the H I of the galaxy ends, and the more extended H I envelope begins. The large beams with which H I is typically observed exacerbate the problem, both because of beam dilution which causes H I surface density to be underestimated, but also because the tiny dimensions of the galaxies compared with their H I envelope make it difficult to assess the H I content of the galaxy itself.

Because our interest here is in dust production, and in the cool gas reservoir that provides the fuel for star formation, we have taken H I surface densities from the highest-resolution observations available (as in H14), and calculated H I mass over the optical extent of the galaxy as determined from (*V*-band) surface-brightness profiles. The *V*-band brightness profile of IZw 18 falls to 25 mag arcsec⁻² at a radius of ~ 8 arcsec (700 pc, Hunt et al. 2003), and a radius $\sim 3/2$ for SBS 0335–052 (838 pc, Thuan et al. 1997). With mean H I surface densities $\Sigma_{\text{HI}} = 56 M_{\odot} \text{pc}^{-2}$ for SBS 0335–052 (Thuan & Izotov 1997) and $64 M_{\odot} \text{pc}^{-2}$ for IZw 18 (Lelli et al. 2012), we thus estimate total H I masses of $3.1 \times 10^7 M_{\odot}$ and $2.5 \times 10^7 M_{\odot}$ for SBS 0335–052 and IZw 18, respectively. The H I mass for SBS 0335–052 is about 10 times lower than the total H I mass by Ekta et al. (2009) in a 40 arcsec beam (about 6 times larger than the optical extent of the galaxy), and ~ 4 times lower than the total for IZw 18 given by Lelli et al. (2012). Using the total H I masses from the literature would lower the resulting DGR by roughly these amounts (e.g., Rémy-Ruyer et al. 2014).

¹ This assumption is almost certainly inexact, but provides a benchmark for our assessment of consistency with observations.

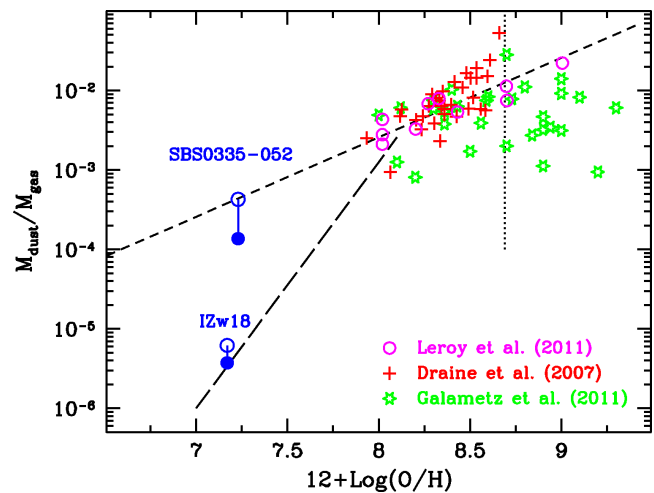


Figure 1. Dust-to-gas mass ratios (DGRs) as a function of metallicity. Filled (blue) circles show DGRs inferred from the total gas mass of SBS 0335–052 and IZw 18, including ionized gas, atomic and (putative, as yet undetected) molecular gas; open circles give DGRs including only the ionized and atomic gas components. Galaxies from Galametz et al. (2011) are shown as (green) open stars, those from Draine et al. (2007) as (red) crosses, and from Leroy et al. (2011) as (magenta) open circles. The short dashed line is the linear prediction by Draine et al. (2007), and the vertical dotted line illustrates solar metallicity $12 + \log(\text{O}/\text{H}) = 8.69$ (Asplund et al. 2009). The long dashed line (starting at $12 + \log(\text{O}/\text{H}) = 8.0$) is the empirical fit given by Rémy-Ruyer et al. (2014) for low metallicities.

2.2 Ionized gas masses

In low-metallicity star-forming galaxies such as IZw 18 and SBS 0335–052, ionized gas constitutes an important part of the total gas mass budget. Hence, we have attempted to determine the mass of the ionized component in the two galaxies.

Radio continuum observations of the free-free emission of ionized gas give emission measures, and thus mean densities and source size. The radio spectrum for IZw 18 is flat, consistent with optically thin emission (Cannon et al. 2005; Hunt et al. 2005b), while that of SBS 0335–052 falls at low frequency, indicative of free-free absorption and consequently high ionized-gas density (Hunt et al. 2004; Johnson et al. 2009). As discussed in detail in Sect. 2.6, the density of ionized gas in IZw 18 is $\sim 5 \text{cm}^{-3}$, and $\sim 3200 \text{cm}^{-3}$ in SBS 0335–052, corresponding to emitting regions of ~ 390 pc radius for IZw 18 (Hunt et al. 2005b) and ~ 7.7 pc radius for SBS 0335–052 (Johnson et al. 2009).

Because ionized gas tends to be clumped (Kassim et al. 1989; Kennicutt 1984; Zaritsky et al. 1994; Martin 1997; Giammanco et al. 2004; Cormier et al. 2012; Lebouteiller et al. 2012), we need to estimate a volume filling factor over the optical extent of the galaxy. We have done this by comparing the source size inferred from the radio emission measure to the optical size (see Sect. 2.1), assuming a spherical geometry for the H II region. This comparison gives a volume filling factor of 0.17 for IZw 18 and $\sim 10^{-6}$ for SBS 0335–052. Although the value for IZw 18 is within those observed for local H II regions (e.g., Kassim et al. 1989), the value for SBS 0335–052 is extremely low. This could be a consequence (e.g., Giammanco et al. 2004) of the optically thick gas in this galaxy as indicated by the radio spectrum, so for SBS 0335–052 we have used conservatively a filling factor of 3×10^{-4} , roughly the lowest value found by Martin (1997). With these densities and filling

factors, and the optical size of the galaxy as for H1, we estimate ionized gas masses of $3.1 \times 10^7 M_\odot$ and $5.9 \times 10^7 M_\odot$ for IZw 18 and SBS 0335–052, respectively. The mass of the ionized gas is comparable to that of the atomic gas in both galaxies.

If, instead of the radio-determined value of 3200 cm^{-3} , we consider the ionized gas density of 500 cm^{-3} for SBS 0335–052 inferred from the optical [S II] lines (Izotov et al. 1999), and a larger filling factor of 10^{-3} , we would estimate an ionized gas density of $3 \times 10^7 M_\odot$, 50% of our former estimate. This can be considered as a rough measure of the uncertainty inherent in this calculation.

2.3 Molecular gas masses

CO emission has never been detected in either galaxy; thus it is difficult to measure H_2 masses, independently of the unknown CO luminosity-to- H_2 mass conversion factor α_{CO} . Thus, H14 measured the distance from the gas scaling relations in order to estimate the missing (undetected) H_2 gas surface density (for more details, see H14). Using the densities from H14 ($\Sigma_{\text{H}_2} = 94 M_\odot \text{ pc}^{-2}$ and $\Sigma_{\text{H}_2} = 342 M_\odot \text{ pc}^{-2}$, for IZw 18 and SBS 0335–052, respectively) and the optical size of the galaxy as above, we infer H_2 masses for IZw 18 and SBS 0335–052 of $3.6 \times 10^7 M_\odot$ and $1.9 \times 10^8 M_\odot$, respectively. These masses are highly uncertain, and assume that SFR surface density at low metallicity follows the same scaling relations as more metal-enriched galaxies.

2.4 Dust masses and comparison with previous work

Dust masses for SBS 0335–052 and IZw 18 were measured by H14 by fitting the optical-to-mm spectral energy distributions (SEDs) with spherical *DUSTY* models (Ivezic & Elitzur 1997). Three different grain populations were included for determination of the best-fit model (for more details see H14). The resulting dust masses for both galaxies differ from those measured by other groups (e.g., Rémy-Ruyer et al. 2013; Fisher et al. 2014; Rémy-Ruyer et al. 2014; Izotov et al. 2014). H14 discussed differences relative to Rémy-Ruyer et al. (2013) for SBS 0335–052 and Fisher et al. (2014) for IZw 18; here we compare our measurements to more recent work although we are unable to compare our dust-mass estimates with Rémy-Ruyer et al. (2014) because there is no tabulation of their dust masses.

Izotov et al. (2014) use a multiple-temperature modified blackbody (MBB) approach, and fix the emissivity index for all components. However, they only discuss the warm and cold dust (not the hot) because, as they note, the hot dust (for $\lambda < 10 \mu\text{m}$) is not in thermal equilibrium. Considering their two-component fits, the SEDs shown in their Fig. 6 almost never pass through the longer wavelength points. This is a consequence of the assumption of single-temperature MBBs, and is expected to bias dust-mass estimates toward lower masses. Although seemingly a small deviation, the constraints offered by longer wavelengths significantly raise dust mass estimates, especially at low metallicity (e.g., Galametz et al. 2011). It is well known that including short wavelengths in a single-temperature MBB fit gives unrealistically low dust masses because the mean temperature of the dust radiating at these short wavelengths is higher than the bulk of the cooler dust which dominates the mass. The warm dust dominates the light but the cool dust dominates the mass and a single temperature (or even two temperatures as in Izotov et al. 2014) are not able to accommodate the temperature gradients.

The cold-dust mass found by Izotov et al. (2014) for IZw 18

is 70% of that found by H14; compensating for the differences in dust emissivities worsens slightly the discrepancy to $\sim 65\%$. This value is also a factor of 2 below the lower limit of the range of dust mass estimated for IZw 18 by Fisher et al. (2014) who use models by Draine & Li (2007), even after compensating for the different emissivities adopted by the two groups. More physically realistic models which contemplate dust temperature gradients through variations in the interstellar radiation field that heats the dust tend to give larger dust masses than single-temperature MBB fits.

For SBS 0335–052, Izotov et al. (2014) find a cold dust mass of dex $3.06 M_\odot$, roughly a factor of 30 below H14. However, they estimate a “cold” temperature of 57 K, very close to the temperature of 59 K discussed by H14 under the assumption of single-temperature dust, and thus do not take into account any cool dust. Moreover, the dust in SBS 0335–052 is optically thick at short wavelengths (Thuan et al. 1999; Plante & Sauvage 2002; Houck et al. 2004; Hunt et al. 2005a, 2014); thus the assumption of optically thin dust emission implicit in MBB fitting is incorrect.

The differences found in dust masses for SBS 0335–052 and IZw 18 of roughly a factor of 100 are consistent with the differences in their integrated IR luminosity: L_{IR} for SBS 0335–052 is $1.6 \times 10^9 L_\odot$, while for IZw 18 $L_{\text{IR}} = 2 \times 10^7 L_\odot$. Assuming the same mass-to-light ratio (similar overall mean temperatures) for the dust, this would give a factor of 80 in dust mass, inconsistent with the difference found by Izotov et al. (2014) of roughly a factor of 5 for the cold dust masses in the two galaxies. This illustrates one of the difficulties of the MBB approach adopted by Izotov et al. (2014); they use two temperatures and thus apply two different mass-to-light ratios (roughly inverse temperature) to the two IR integrals. As mentioned above, in galaxies like SBS 0335–052 and IZw 18 most of the dust *emission* comes from warm dust, while most of the dust *mass* is cold.

More emissive grain mixtures, as suggested by Jones et al. (2013), would decrease the inferred dust mass by a factor 3–4 in both galaxies. A comparable reduction of the dust mass of SBS 0335–052 ($\sim 9 \times 10^3 M_\odot$) would be obtained by artificially imposing a low $870 \mu\text{m}$ dust flux (1σ below the reported H14 flux).

We will discuss the implication of this reduction in dust mass for our results in Sect. 3.

Figure 1 shows the DGRs of IZw 18 and SBS 0335–052, together with samples of galaxies taken from the literature (with dust masses obtained through SED fitting rather than MBB approximations). Because the dust-mass estimates for these samples are based on the Draine & Li (2007) models, the dust emissivities are comparable among the samples. Figure 1 also shows the steeper-than-linear slope found by Rémy-Ruyer et al. (2014) for galaxies with oxygen abundance $12 + \log(\text{O}/\text{H}) \leq 8.0$. The DGR of SBS 0335–052 is roughly consistent with a linear slope of DGR with O/H (e.g., Draine et al. 2007), while IZw 18 follows the steeper slope found by Rémy-Ruyer et al. (2014).

2.5 Stellar masses, stellar ages, and SFR

Stellar masses in star-forming dwarf galaxies such as SBS 0335–052 and IZw 18 are notoriously difficult to determine. The main problem is contamination by nebular continuum emission which affects both the optical (e.g., Reines et al. 2008, 2010; Adamo et al. 2010) and the near-infrared emission (e.g., Smith & Hancock 2009; Hunt et al. 2012). In SBS 0335–052, the contamination from free-free emission at $3.4 \mu\text{m}$ is 27% (Hunt et al. 2001) and $\sim 50\%$ at $2.2 \mu\text{m}$ (Vanzi et al. 2000); even more extreme contamination is observed in IZw 18, with $>50\%$ of the

Table 1. Adopted physical properties of the two galaxies. The SFR values are from radio-continuum SED fitting. The stellar ages are the mean values of stellar clusters and the stellar masses have been derived integrating the SFR over the mean ages (see text). The values in parentheses correspond to those from *DUSTY* SED fitting (stellar mass, stellar age, metallicity, dust mass) and to a constant SFR inferred from the *DUSTY* SED best-fit stellar mass and ages.

Name	Distance (Mpc)	Gas Component	M_{gas} ($10^7 M_{\odot}$)	M_{star} ($10^6 M_{\odot}$)	SFR ($M_{\odot} \text{ yr}^{-1}$)	Age (Myr)	12+ Log(O/H) ^a	Z ($10^{-2} Z_{\odot}$)	M_{dust} ($10^2 M_{\odot}$)	n_{mol} (cm^{-3})	T_{mol} (K)
IZw 18	18.2	Ionized	3.07								
		Atomic	2.46								
		Molecular ^b	3.62								
		Total	9.15	1.02 (1.82)	0.17 (0.10)	6 (18.3)	7.18	3.09 (2)	(3.4 ± 1)	100	10
SBS 0335–052	54.1	Ionized	5.85								
		Atomic	3.09								
		Molecular ^b	18.9								
		Total	27.8	7.92 (23.5)	1.32 (1.79)	6 (13.1)	7.27	3.80 (2)	(3.8 ± 0.6) × 10 ²	1500	80

^a Averages taken from Izotov et al. (1999).

^b H₂ surface densities inferred by H14 from gas scaling relations, not directly detected. See text for more details.

IRAC 4.5 μm flux due to nebular emission (Hunt et al. 2012). Hot dust is also a problem, especially in SBS 0335–052 where it comprises $\sim 67\%$ of its 4 μm emission (Hunt et al. 2001). While nebular continuum levels can be estimated from SFRs (e.g., Smith & Hancock 2009; Hunt et al. 2012), it is difficult to ascertain hot-dust levels without detailed multi-wavelength photometry. Thus stellar masses of low-metallicity dwarf starbursts such as SBS 0335–052 and IZw 18 are prone to large uncertainties.

Table 1 reports in parentheses the values of stellar mass, M_{star} , and age inferred from *DUSTY* SED fitting (H14), and SFRs that correspond to the constant values needed to produce the *DUSTY* SED best-fit M_{star} when integrated over the best-fit age. However, for our analysis, we require a *mean* age for the stellar populations producing the dust currently observed. A mean age of stellar clusters of 6 Myr has been calculated by averaging values from Recchi et al. (2002) and Hunt et al. (2003) for IZw 18 and from Reines et al. (2008) for SBS 0335–052. Thus, we have also computed the stellar mass accumulated over the timespan of the mean ages of the clusters at a constant rate given by the observed values of SFR derived from radio free-free emission (Hunt et al. 2005b; Johnson et al. 2009). All these values (not in parentheses) are also reported in Table 1.

The resulting M_{star} values are within 40% of previous estimates obtained by fitting the optical-NIR SEDs of individual star clusters with single stellar population models (SBS 0335–052: $5.6 \times 10^6 M_{\odot}$, IZw 18: $7.0 \times 10^5 M_{\odot}$, Reines et al. 2008; Fumagalli et al. 2010, respectively).

Only if age priors (3–6 Myr) are imposed for the fit are the *DUSTY* stellar masses obtained by H14 consistent with these values for SBS 0335–052. There is a similar discrepancy for the *DUSTY* stellar mass of IZw 18 at an age of 18.3 Myr, almost a factor 2 larger than the value obtained with a constant SFR of $0.17 M_{\odot} \text{ yr}^{-1}$. Part of the reason for this is that, at a given luminosity, the mass-to-light ratios are smaller for younger stellar populations (see H14 for details). Another reason is that there is an age gradient in both galaxies, and the SED fitting relies on global photometry that encompasses both young and old clusters. In SBS 0335–052, the northern super-star clusters (SSCs) are older with a maximum age of ~ 12 Myr, compared to $\lesssim 3$ Myr for the southern ones (Reines et al. 2008; Adamo et al. 2010); in IZw 18, the SE cluster and C component are older ($\sim 10 - 15$ Myr) compared to the younger NW cluster (~ 3 Myr, Hunt et al. 2003).

Such a difference in the stellar ages can have important implications for the chemical evolution of the system. In Fig. 2 we

show the stellar mass-lifetime relation for stars with initial metallicity $Z/Z_{\odot} = 0.03$, using the Raiteri et al. (1996) formulation. The shaded regions illustrate the ranges of stellar masses that contribute to metal enrichment by means of core-collapse SN explosions and stellar winds from intermediate mass stars. The vertical grey lines indicate the values of stellar ages shown in the table (dashed lines are the *DUSTY* stellar ages). The figure shows that part of the metals and dust that we presently observe may have originated *in situ*, from supernova explosions (*self-enrichment* scenario). However, if we adopt the mean age of the stellar clusters (solid line), only the most massive supernovae with $34 M_{\odot} \leq m \leq 40 M_{\odot}$ have evolved to their metal production stage. Hence the ISM of the galaxies must have achieved most of its metal content prior to the current star-formation episode (*pre-enrichment* scenario). If, instead, the stellar population age for SBS 0335–052 (IZw 18) is 13.1 Myr (18.3 Myr), as inferred from *DUSTY* SED fit, then the mass range of the stars that can contribute to the ISM enrichment extends to $16 M_{\odot} \leq m \leq 40 M_{\odot}$ ($13 M_{\odot} \leq m \leq 40 M_{\odot}$).

Fig. 3 quantifies this difference in terms of the mass of metals and dust that can be produced by self-enrichment. It shows that – depending on the adopted stellar age – the mass fraction of metals (dust) relative to the stellar mass is in the range $1.5 \times 10^{-3} \leq Y_Z \leq 7 \times 10^{-3}$ ($3.26 \times 10^{-6} \leq Y_d \leq 6.2 \times 10^{-5}$) for SBS 0335–052 and in the range $1.5 \times 10^{-3} \leq Y_Z \leq 7.9 \times 10^{-3}$ ($3.26 \times 10^{-6} \leq Y_d \leq 8.6 \times 10^{-5}$) for IZw 18. Using the corresponding stellar masses reported in Table 1, we find that – even assuming that all the newly formed dust injected in the ISM is conserved – the dust mass produced by self-enrichment is always smaller than observed, being $26 M_{\odot} \leq M_d \leq 1460 M_{\odot}$ for SBS 0335–052 and $3 M_{\odot} \leq M_d \leq 157 M_{\odot}$ for IZw 18. As explained below, these values have been obtained using the dust and metal yields presented by Valiante et al. (2009) and assuming that the stars form at a constant rate with a Salpeter Initial Mass Function (IMF) in a mass range $0.1 M_{\odot} \leq m \leq 100 M_{\odot}$ with a metallicity of $Z = 0.03 Z_{\odot}$.

2.6 Cold gas densities and temperatures

The remaining quantities required for our models are the mean density and temperature of the cold neutral medium (CNM) and molecular clouds in which dust grains form and grow by accretion (see Sect. 3). We can derive the number densities of the molecular phase by assuming thermal pressure balance at the atomic-molecular interface (e.g., Krumholz et al. 2009a). Observationally and from a theoretical point of view, the mean number density of molecu-

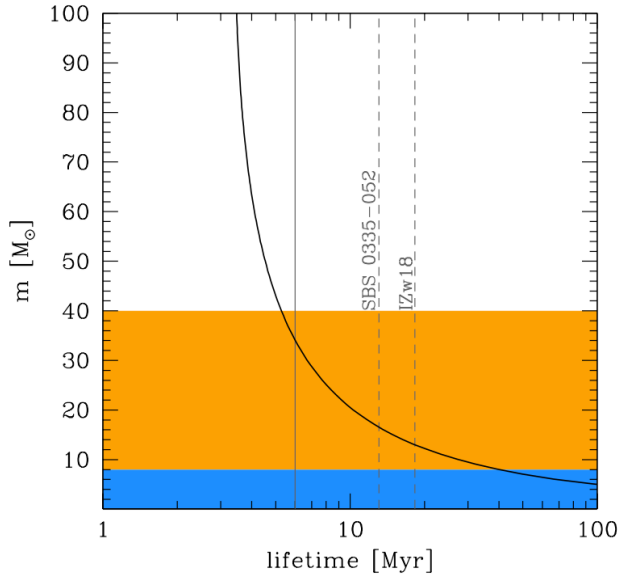


Figure 2. The dependence of the stellar lifetime on the initial stellar mass for stars with metallicity $Z/Z_{\odot} = 0.03$ (solid black line). The orange and blue regions indicate the progenitor mass ranges of core-collapse SN and AGB stars, respectively. The solid and dashed vertical lines indicate the estimated stellar ages for the two galaxies, based on individual super stellar clusters fits and on *DUSTY* SED fits, respectively (see text).

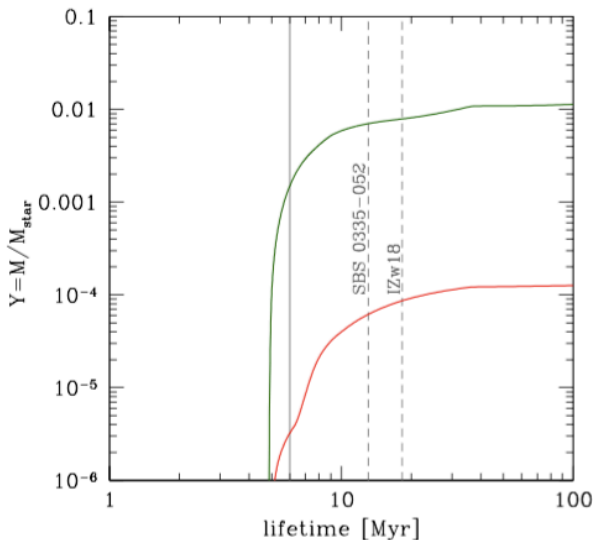


Figure 3. The mass fraction of metals (dark green) and dust (red) relative to the mass of stars as a function of the stellar age. The solid and dashed vertical lines indicate the estimated stellar ages for the two galaxies, based on individual super stellar clusters fits and on *DUSTY* SED fits, respectively (see text).

lar clouds, $\langle n_{\text{mol}} \rangle$, is expected to be $\phi_{\text{mol}} \sim 10$ times that in the CNM of the ISM: $\langle n_{\text{mol}} \rangle = \phi_{\text{mol}} \langle n_{\text{CNM}} \rangle$. We can therefore calculate approximate values of n_{mol} in SBS 0335–052 and IZw 18 by

first considering the observed H I column densities²: $7 \times 10^{21} \text{ cm}^{-2}$ and $4.8 \times 10^{21} \text{ cm}^{-2}$ for SBS 0335–052 and IZw 18, respectively (Thuan & Izotov 1997; Lelli et al. 2012). These can be converted to mean volume densities over the regions of interest (the area subtended by the massive star clusters) by considering the diameters of the star-forming region: $\sim 15.8 \text{ pc}$ for SBS 0335–052 (Johnson et al. 2009) and $\sim 170 \text{ pc}$ for IZw 18 (Cannon et al. 2002; Hunt & Hirashita 2009). We thus obtain a mean molecular density $\langle n_{\text{mol}} \rangle \sim 1435 \text{ cm}^{-3}$ and $\langle n_{\text{mol}} \rangle \sim 91 \text{ cm}^{-3}$ for SBS 0335–052 and IZw 18, respectively.

Despite the similar metallicities of the two galaxies, the inferred molecular densities differ by more than an order of magnitude. Nevertheless, these estimates are roughly consistent, given the uncertainties, with the densities that would be inferred from the putative (unobserved) molecular component discussed by H14. Assuming that the Kennicutt-Schmidt law relating gas and star-formation surface densities holds also for these two galaxies, and with the same sizes as above, we would derive $\langle n_{\text{mol}} \rangle \sim 1800 \text{ cm}^{-3}$ for SBS 0335–052 and $\langle n_{\text{mol}} \rangle \sim 40 \text{ cm}^{-3}$ for IZw 18. The radio spectrum also shows evidence for such a difference in gas densities in the two galaxies. While in SBS 0335–052 there is the clear signature of a strongly absorbed thermal component, both globally (Hunt et al. 2004) and around the individual southern SSCs (Johnson et al. 2009), IZw 18 shows a typical flat bremsstrahlung spectrum (Hunt et al. 2005b). Based on fits of the radio spectrum, the ionized-gas densities inferred for the two objects are $\sim 3200 \text{ cm}^{-3}$ for SBS 0335–052 (Johnson et al. 2009), and $< 10 \text{ cm}^{-3}$ for IZw 18 (Hunt et al. 2005b). Finally, even the optical spectra of the two objects show a large difference in the densities measured from the [S II] lines: $\geq 500 \text{ cm}^{-3}$ for SBS 0335–052 and $\leq 100 \text{ cm}^{-3}$ for IZw 18 (Izotov et al. 1999). Given the uncertainties in the above estimates, in what follows we take the reference values of 1500 cm^{-3} and 100 cm^{-3} for the molecular gas densities in SBS 0335–052 and IZw 18, respectively.

Following Krumholz et al. (2009a), we can use the temperature-density relation for the CNM predicted by Wolfire et al. (2003) ISM model³ to find T_{CNM} and then derive the temperature of the molecular gas implied by thermal pressure balance, $T_{\text{mol}} = 1.8 T_{\text{CNM}} / \phi_{\text{mol}}$. The resulting values for the two galaxies are shown in Table 1.

3 THE CHEMICAL EVOLUTION MODEL

The equations describing the chemical evolution of a galaxy that evolves in isolation (closed-box approximation), can be summarized as follows:

$$\dot{M}_{\text{star}}(t) = \text{SFR}(t) - \dot{R}(t), \quad (1)$$

$$\dot{M}_{\text{ISM}}(t) = -\text{SFR}(t) + \dot{R}(t) \quad (2)$$

$$\dot{M}_{\text{Z}}(t) = -Z_{\text{ISM}}(t)\text{SFR}(t) + \dot{Y}_{\text{Z}}(t) \quad (3)$$

$$\begin{aligned} \dot{M}_{\text{d}}(t) = & -Z_{\text{d}}(t)\text{SFR}(t) + \dot{Y}_{\text{d}}(t) \\ & -(1 - X_{\text{c}}) \frac{M_{\text{d}}(t)}{\tau_{\text{d}}} + X_{\text{c}} \frac{M_{\text{d}}(t)}{\tau_{\text{acc}}} \end{aligned} \quad (4)$$

² We have considered regions of similar size, constrained by requiring a similar physical resolution of the H I observations: $\sim 524 \text{ pc}$ ($2''$) for SBS 0335–052 and $\sim 436 \text{ pc}$ ($5''$) for IZw 18.

³ We have considered the most general expression for the CNM temperature, which takes into account the vastly different DGRs for these two galaxies.

where M_{star} is the stellar mass, M_{ISM} is the total mass in the ISM (the sum of the gas and dust masses), M_Z is the total mass in heavy elements (both in the gas phase and in dust grains), M_d is the dust mass (so that the mass of gas phase elements is given by $M_{\text{met}} = M_Z - M_d$), $Z_{\text{ISM}}(t) = M_Z(t)/M_{\text{ISM}}(t)$ is the ISM metallicity, and $Z_d(t) = M_d(t)/M_{\text{ISM}}(t)$ is the total dust abundance in the ISM. The terms $\dot{R}(t)$, $\dot{Y}_Z(t)$ and $\dot{Y}_d(t)$ are the rates at which the mass of gas, heavy elements and dust is returned to the ISM after stellar evolution, respectively. These time-dependent terms depend on the adopted model grids and stellar IMF. We compute them as follows:

$$\dot{R}(t) = \int_{m(t)}^{m_{\text{up}}} (m - m_r(m, Z)) \Phi(m) \text{SFR}(t - \tau_m) dm, \quad (5)$$

$$\dot{Y}_Z(t) = \int_{m(t)}^{m_{\text{up}}} m_Z(m, Z) \Phi(m) \text{SFR}(t - \tau_m) dm, \quad (6)$$

$$\dot{Y}_d(t) = \int_{m(t)}^{m_{\text{up}}} m_d(m, Z) \Phi(m) \text{SFR}(t - \tau_m) dm, \quad (7)$$

where the lower limit of integration, $m(t)$, is the mass of a star with a lifetime $\tau_m = t$; m_r , m_Z , and m_d are respectively the remnant mass, the metal and dust mass yields, which depend on the stellar mass and metallicity; and $\Phi(m)$ is the stellar IMF, which we assume to be a Salpeter law in the mass range $0.1 M_{\odot} \leq m \leq 100 M_{\odot}$ (e.g., Valiante et al. 2009). For stars with $m < 8 M_{\odot}$, we adopt metal yields from van den Hoek & Groenewegen (1997) and dust yields for intermediate-mass stars on the AGB phase of the evolution by Zhukovska et al. (2008). For massive stars ($12 M_{\odot} < m < 40 M_{\odot}$) metal and dust yields have been taken from Woosley & Weaver (1995) and from Bianchi & Schneider (2007), using the proper mass- and metallicity-dependent values and including the effect of the reverse shock on dust survival in SN ejecta. For stars in the intermediate mass range $8 M_{\odot} \leq m \leq 12 M_{\odot}$, we interpolate between the AGB yields for the largest-mass progenitor and SN yields from the lowest-mass progenitor. Above $40 M_{\odot}$, stars are assumed to collapse to black hole without contributing to the enrichment of the ISM. Finally, the last two terms in the right-hand side of eq. (4) represent the effects of dust destruction by interstellar shock waves and grain growth in the dense phase of the ISM. Here we simplify the treatment of the two-phase ISM model described in de Bressan et al. (2014), and quantify the fraction of ISM in the cold phase with the parameter X_c . This is taken to be time-dependent and rescaled from the SFR,

$$\text{SFR}(t) = \frac{\epsilon_* X_c(t) M_{\text{gas}}(t)}{\tau_{\text{ff}}}, \quad (8)$$

where ϵ_* is the star formation efficiency (Krumholz et al. 2012),

$$\tau_{\text{ff}} = \sqrt{\frac{3\pi}{64 G m_{\text{H}} < n_{\text{mol}} >}} \quad (9)$$

is the free-fall timescale at the mean density of molecular clouds $< n_{\text{mol}} > \gg 2 m_{\text{H}} < n_{\text{mol}} >$. Finally, the timescale for grain destruction, τ_d and grain growth τ_{acc} are computed as in de Bressan et al. (2014). The latter timescale depends on the gas phase metallicity, temperature and density of molecular clouds,

$$\tau_{\text{acc}} = 20 \text{ Myr} \times \left(\frac{n_{\text{mol}}}{100 \text{ cm}^{-3}} \right)^{-1} \left(\frac{T_{\text{mol}}}{50 \text{ K}} \right)^{-1/2} \left(\frac{Z}{Z_{\odot}} \right)^{-1} \quad (10)$$

where we have assumed that grains which experience grain growth have a typical size of $\sim 0.1 \mu\text{m}$ (Hirashita & Voshchinnikov 2014). If $n_{\text{mol}} = 10^3 \text{ cm}^{-3}$ and $T_{\text{mol}} = 50 \text{ K}$, the accretion timescale for gas at solar metallicity is only 2 Myr (Asano et al. 2013).

Below we apply the chemical evolution model to each of the two galaxies under investigation. Throughout the following, we adopt a solar metallicity of $Z_{\odot} = 0.0134$ (Asplund et al. 2009).

3.1 SBS 0335–052

The observed mass of metals in SBS 0335–052 is $M_{\text{met}}(t_{\text{obs}}) = Z M_{\text{gas}}(t_{\text{obs}}) = [4.53 \times 10^4 - 1.41 \times 10^5] M_{\odot}$ (the lower limit corresponds to pure atomic gas and the upper one to the total gas mass, see Table 1). The observed dust mass is $M_{\text{dust}}(t_{\text{obs}}) = 3.8 \times 10^4 M_{\odot}$. Hence, the total mass in heavy elements $M_Z(t_{\text{obs}})$ ranges from $8.33 \times 10^4 M_{\odot}$ to $1.79 \times 10^5 M_{\odot}$. As described in Sect. 2, the maximum dust mass that can be produced by self-enrichment from observed stellar populations in SBS 0335–052 is $\sim 1.5 \times 10^3 M_{\odot}$, ~ 25 times lower than the estimated dust mass reported in Table 1 (Hunt et al. 2014) and $\sim 50\%$ lower than the lowest limit on the dust mass reported by Thuan et al. (1999). It is therefore unlikely that the origin of the dust in SBS 0335–052 is self-enrichment. In fact, the same stars responsible for metal pre-enrichment may have also formed dust. Alternatively, the dust mass may have formed *in situ* by means of grain growth. We examine each of these two possibilities in turn.

We first assume that the stars observed in SBS 0335–052, with a total mass of $M_{\text{star}} = 7.92 \times 10^6 M_{\odot}$, have a mean age of 6 Myr and have formed at a constant rate of $1.32 M_{\odot}/\text{yr}$ with a Salpeter IMF (see the values in Table 1). Under these conditions, only stars with masses $m \geq 34 M_{\odot}$ had the time to evolve and the total mass of heavy elements and dust injected in the ISM by SNe is $1.18 \times 10^4 M_{\odot}$ and $25.8 M_{\odot}$, respectively, much smaller than observed. From eq. (3), we can estimate the mass of metals that was originally present in SBS 0335–052, $M_Z(t_{\text{ini}})$, where $t_{\text{ini}} = t_{\text{obs}} - 6 \text{ Myr}$. This is equal to the mass presently observed, corrected for astration and self-enrichment,

$$M_Z(t_{\text{ini}}) = M_Z(t_{\text{obs}}) - \int_{t_{\text{ini}}}^{t_{\text{obs}}} dt [-Z_{\text{ISM}}(t) \text{SFR}(t) + \dot{Y}_Z(t)], \quad (11)$$

and we find $M_Z(t_{\text{ini}}) \sim 1.79 \times 10^5 M_{\odot}$. Assuming the Salpeter IMF-averaged dust and metal yields for a fully-evolved stellar population with a metallicity $Z = 0.03 Z_{\odot}$ ($Y_Z = 1.43 \times 10^{-2}$ and $Y_d = 4.6 \times 10^{-4}$), the maximum mass of dust that SBS 0335–052 could have achieved by pre-enrichment can be estimated as

$$M_d(t_{\text{ini}}) = \frac{Y_d}{Y_Z} M_Z(t_{\text{ini}}) \sim 5.7 \times 10^3 M_{\odot}, \quad (12)$$

which is only $\sim 15\%$ of the observed value.

We can repeat the same calculation but assuming that the observed stars in SBS 0335–052 have a mean age of 13.1 Myr, a total stellar mass of $M_{\text{star}} = 2.35 \times 10^7 M_{\odot}$ and have formed with a constant SFR of $1.79 M_{\odot}/\text{yr}$ with a Salpeter IMF (see the values in parenthesis in Table 1). In this case, newly formed stars with masses $m \geq 16 M_{\odot}$ produce $1.65 \times 10^5 M_{\odot}$ of heavy elements and $1460 M_{\odot}$ of dust, too small to account for the observed dust mass. Using eq. (11), we find that the mass of heavy elements achieved by means of pre-enrichment at $t_{\text{ini}} = t_{\text{obs}} - 13.1 \text{ Myr}$ is $M_Z(t_{\text{ini}}) \sim 1.56 \times 10^5 M_{\odot}$, which corresponds to a maximum dust mass of $M_d(t_{\text{ini}}) \sim 5 \times 10^3 M_{\odot}$ (from eq. 12), $\sim 13\%$ of the observed value.

It is important to stress that the above values of $M_d(t_{\text{ini}})$ should be regarded as upper mass limits. In fact, if we were to consider only the atomic gas rather than the total (including the putative molecular component), the dust masses allowed by pre-enrichment would be even lower, $\lesssim 10\%$ in both cases. Moreover, eq. (12)

is based on the implicit assumption that all the dust produced by previous stellar generations has been conserved in the ISM, without undergoing any destruction by interstellar shocks. Hence, pre-enrichment cannot account for the observed dust masses, even if we were to consider a factor 3-4 reduction in the observed dust mass, either by using more emissive grain mixtures (Jones et al. 2013), or by artificially lowering the observed 870 μm dust flux in the SED (see Sect. 2.4).

Independently of the adopted stellar ages, a major fraction of the existing mass of dust in SBS 0335–052 must have formed by means of grain growth in the dense phase of the ISM.

In Figure 4 we show the results of chemical evolution models. Since it is impossible to constrain the initial value of dust mass that SBS 0335–052 has inherited from previous stellar generations, we have explored two limiting cases: in the first one, we take the observed gas density of $\langle n_{\text{mol}} \rangle \sim 1500 \text{ cm}^{-3}$ (see Table 1) and we start from the minimum initial dust mass that allows the model to reproduce the observations (red shaded region between the two solid lines). This model shows that if the stellar age is 6 Myr, SBS 0335–052 must start with the maximum possible initial dust mass predicted by eq. (12), grain growth accounts for $\sim 85\%$ of the existing dust mass, with pre-enrichment providing the remaining $\sim 15\%$. If the stellar age is 13.1 Myr, due to the longer time available for grain growth, SBS 0335–052 can start with a dust mass that is $\sim 30\%$ of the maximum value achieved by pre-enrichment and grain growth accounts for $\sim 95\%$ of the observed dust mass. In the second model (blue shaded region between the two shaded lines), we assume an initial dust mass of only $1 M_{\odot}$, as if the chemical initial conditions inherited from previous stellar generations were not favourable to dust pre-enrichment. Under this pessimistic scenario, a gas density of $n_{\text{mol}} = 10^4 \text{ cm}^{-3}$ ($5 \times 10^3 \text{ cm}^{-3}$) would allow grain growth to increase the dust mass, reaching the observed value in 6 Myr (13.1 Myr). The above results have been obtained solving the system of equations (1) - (4) assuming an initial gas mass $M_{\text{gas}}(t_{\text{ini}}) = M_{\text{gas}}(t_{\text{obs}}) + M_{\text{star}}(t_{\text{obs}})$ (closed-box approximation) and fixing the free parameters X_{c} and ϵ_{*} to reproduce the mass of molecular gas component at t_{obs} . For $\langle n_{\text{mol}} \rangle \sim 1500 \text{ cm}^{-3}$ this constrains the star formation efficiency to be $7 \times 10^{-3} \leq \epsilon_{*} \leq 9 \times 10^{-3}$ and the fraction of molecular gas to be $X_{\text{c}} = 0.67$.

Hence we conclude that, provided that a major fraction of the dense gas in SBS 0335–052 is at densities $1.5 \times 10^3 \text{ cm}^{-3} < n_{\text{mol}} < 10^4 \text{ cm}^{-3}$, the observed dust mass in SBS 0335–052 can be reproduced by means of grain growth.

3.2 IZw 18

We next analyse the evolution of IZw 18. The observed mass of metals and dust are $M_{\text{met}}(t_{\text{obs}}) = Z M_{\text{gas}}(t_{\text{obs}}) = [2.29 - 3.78] \times 10^4 M_{\odot}$ (the lower limit corresponds to pure atomic gas and the upper one to the total gas mass, see Table 1) and $M_{\text{d}}(t_{\text{obs}}) = 3.4 \times 10^2 M_{\odot}$, resulting in a total mass of heavy elements of $M_{\text{Z}}(t_{\text{obs}}) = [2.32 - 3.82] \times 10^4 M_{\odot}$. Depending on the adopted stellar ages ($6 \text{ Myr} \leq t_{\text{age}} \leq 18.3 \text{ Myr}$), between 4 and 60% of the observed metal mass can be achieved by self-enrichment, the remaining fraction must have come from previous stellar generations. The same is true for the dust mass: even assuming that all the dust injected by SNe in the ISM is conserved, self-enrichment can produce between $\lesssim 1$ and $\sim 46\%$ of the existing dust mass. Using eqs. (11) and (12), the initial mass of heavy elements and dust can be estimated to be:

$$M_{\text{Z}}(t_{\text{ini}}) \sim (1.93 - 3.82) \times 10^4 M_{\odot},$$

$$M_{\text{d}}(t_{\text{ini}}) = \frac{Y_{\text{d}}}{Y_{\text{Z}}} M_{\text{Z}}(t_{\text{ini}}) \sim (0.62 - 1.23) \times 10^3 M_{\odot},$$

where the upper (lower) initial values have been obtained assuming a stellar age of 6 (18.3) Myr and considering only atomic versus total gas mass. Because the initial maximum dust masses are a factor 2–4 larger than the observed value, all of the existing dust mass in IZw 18 could originate from dust pre-enrichment.

Figure 5 shows the results of chemical evolution models. Similarly to the case of SBS 0335–052, we solve the system of equations (1) - (4) in the closed-box approximation with parameters X_{c} and ϵ_{*} fixed to reproduce the mass of molecular gas component at t_{obs} . We first fix the gas density to its observed value, $\langle n_{\text{mol}} \rangle = 100 \text{ cm}^{-3}$, and we run the model starting from the minimum initial dust mass that allows the observed dust mass to be reproduced (red shaded region between the two solid lines). This implies a star formation efficiency $1.7 \times 10^{-2} \leq \epsilon_{*} \leq 10^{-2}$ and a molecular gas fraction of $X_{\text{c}} = 0.39$. It is clear that grain growth is negligible and that the required initial dust mass is smaller when the stellar age is 18.3 Myr, due to the larger contribution given by self-enrichment. According to this scenario, the system starts with an initial dust mass of $M_{\text{d}}(t_{\text{ini}}) \sim [276 - 338] M_{\odot}$, and then evolves very slowly, with dust injected by newly-formed stars, partly compensated by grain destruction by interstellar shocks and astration. As a result, more than $\sim 80\%$ of the observed dust mass is inherited from pre-enrichment, with grain growth making up the rest. This is different from the solid lines shown in Fig. 4, and a consequence of the lower gas density observed in IZw 18, which causes grain growth to be inefficient. The dashed lines in Fig. 5 show the evolution when – by construction – we impose grain growth to provide the dominant contribution to the final dust mass. In this case, we can start from a negligible initial dust mass but the required gas densities are in the range $9.5 \times 10^3 \text{ cm}^{-3} \leq n_{\text{mol}} \leq 3.75 \times 10^4 \text{ cm}^{-3}$, values which are not supported by observations of any of the gas phases.

4 IMPLICATIONS FOR HIGH-REDSHIFT GALAXIES

The strong dependence of grain growth and the assembly of dust mass on ISM density has profound implications for early galaxy evolution. To date, only one star-forming galaxy at $z > 6$, A1689-zD1 with $z \sim 7.5$, has a clear detection of dust emission (Watson et al. 2015). This galaxy has a (lensing-corrected) stellar mass $M_{\text{star}} \sim 1.7 \times 10^9 M_{\odot}$, and $\text{SFR} \sim 3 - 9 M_{\odot} \text{ yr}^{-1}$. With an estimated dust mass of $4 \times 10^7 M_{\odot}$, the dust-to-stellar mass ratio for this galaxy is relatively high, ~ 0.02 , comparable to the highest values found for local star-forming galaxies at similar masses (e.g., Skibba et al. 2011). The age of A1689-zD1 is estimated to be ~ 80 Myr, at a redshift when the universe was $\lesssim 500$ Myr old.

Despite extensive efforts, dust emission in other star-forming galaxies at comparable redshifts ($z \gtrsim 7$) has not yet been detected (e.g., IOK-1, z8-GND-5296: Ota et al. 2014; Schaerer et al. 2015). Thus, we predict that A1689-zD1 will be found to have a dense ISM, and thus able to assemble a considerable dust mass over the short times available at these redshifts. Our findings suggest that dust mass can be a sensitive indicator of the physical conditions in the ISM, and that metallicity alone is insufficient to determine the amount of dust.

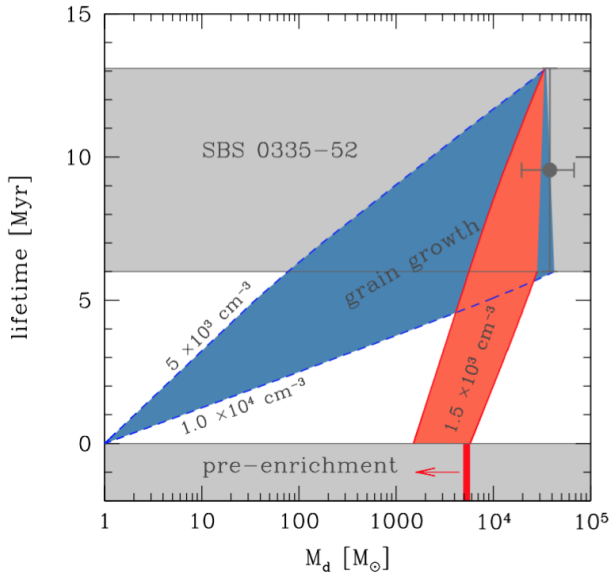


Figure 4. The predicted evolution of the dust mass in SBS 0335–052 is compared with the observed value (grey data point). The upper grey shaded region indicate the range of variation of the inferred stellar ages. The maximum initial dust mass achieved by pre-enrichment is illustrated by the solid red line in the lower grey shaded region. The red region illustrate the range of models where the observed dust mass is reproduced adopting $\langle n_{\text{mol}} \rangle \sim 1500 \text{ cm}^{-3}$ to compute the grain growth timescale and requiring an initial dust mass from pre-enrichment. The blue region illustrate models where dust pre-enrichment is negligible and we adjust the density of dense gas so that the observed dust mass is reproduced by means of grain growth (the required range of n_{mol} is also shown, see text).

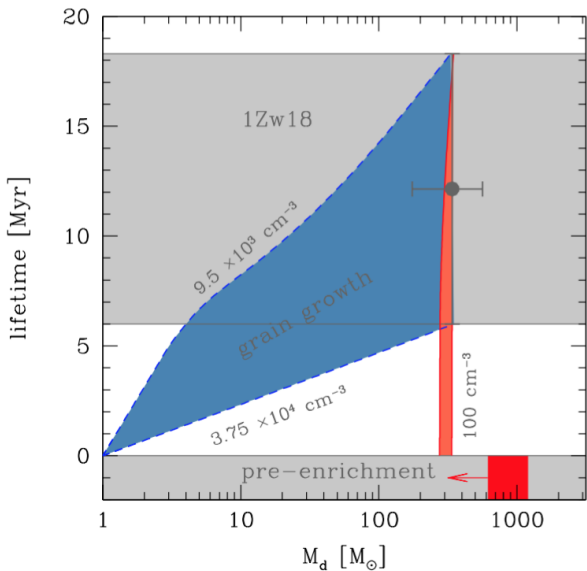


Figure 5. Same as Fig.4 but for IZw 18.

5 CONCLUSIONS

In this paper we have investigated the origin of the observed dust masses in the two most metal-poor local dwarf galaxies, SBS 0335–052 and IZw 18. Despite their comparable metallicities, gas and stellar masses, these two galaxies show a huge vari-

ation in their dust content, with a dust mass of $3.8 \times 10^4 M_{\odot}$ in SBS 0335–052, as inferred by recent ALMA observations (H14), and a dust mass of only $340 M_{\odot}$ in IZw 18. By means of a chemical evolution model with dust, we find that:

- The observed stellar population in SBS 0335–052 can not account for the existing metal and dust masses, hence previous stellar populations must have pre-enriched the ISM of the galaxy.
- Even assuming the maximum possible stellar dust yields, the same stars which have pre-enriched the ISM of SBS 0335–052 could have injected a dust mass which is at most 15% of the observed value. Hence, a major fraction of the observed dust mass must originate *in situ* through grain growth.
- The observed gas density of SBS 0335–052 is large enough to activate efficient grain growth. If $\langle n_{\text{mol}} \rangle = 1500 \text{ cm}^{-3}$, grain growth can account for more than 85% of the existing dust mass, with dust pre-enrichment making up the rest.
- Despite the longer age spread estimated for the stellar population in IZw 18, only between 4 and 60% of the observed metals are produced by self-enrichment through SN explosions of massive stellar progenitors ($m > 13 - 34 M_{\odot}$). Hence, the metallicity has been mostly inherited by previous stellar generations.
- Due to the smaller gas density of IZw 18, grain growth is very inefficient. Since dust injected by newly-formed stars is partly compensated by grain destruction by interstellar shocks and astration, more than 80% of the existing dust mass is inherited from pre-enrichment, with grain growth making up the rest.

Since dust grains can be efficiently destroyed by interstellar shocks, it is very hard to predict the initial mass of dust that can be assembled by pre-enrichment. For this reason, we have also explored a limiting case where the galaxies start with a negligible dust content and achieve all of their dust mass by means of grain growth. This requires the gas density to be larger than inferred from observations: $5 \times 10^3 \text{ cm}^{-3} \leq n_{\text{mol}} \leq 1 \times 10^4 \text{ cm}^{-3}$ for SBS 0335–052 and $9.5 \times 10^3 \text{ cm}^{-3} \leq n_{\text{mol}} \leq 3.75 \times 10^4 \text{ cm}^{-3}$ for IZw 18. While for SBS 0335–052 $n_{\text{mol}} = 5 \times 10^3 \text{ cm}^{-3}$ is within the values estimated by Johnson et al. (2009) for the ionized gas densities (see their Table 4), no observations for IZw 18 suggest similarly high gas densities. However, independently of these considerations, our study suggests that the widely different dust masses in SBS 0335–052 and IZw 18 reflect the different efficiencies of grain growth in their ISM, which – given the comparable metallicity – is likely to originate from the different gas densities of the two galaxies.

ACKNOWLEDGMENTS

We thank Luca Graziani for his insightful comments and Robert Nikutta for a careful analysis of the SED fitting. The research leading to these results has received funding from the European Research Council under the European Unions Seventh Framework Programme (FP/2007-2013) / ERC Grant Agreement n. 306476. LH is grateful to funding from INAF-PRIN 2012/2015.

REFERENCES

- Adamo, A., Zackrisson, E., Östlin, G., & Hayes, M. 2010, *ApJ*, 725, 1620
 Anders, E., & Grevesse, N. 1989, *Geochimica et Cosmochimica Acta*, 53, 197

- Asano, R. S., Takeuchi, T. T., Hirashita, H., & Inoue, A. K. 2013, *Earth, Planets, and Space*, 65, 213
- Asplund, M., Grevesse, N., Sauval, A. J., & Scott, P. 2009, *ARA&A*, 47, 481
- Bianchi, S., & Schneider, R. 2007, *MNRAS*, 378, 973
- Bocchio, M., Jones, A. P., & Slavlin, J. D. 2014, *A&A*, 570, AA32
- Cannon, J. M., Skillman, E. D., Garnett, D. R., & Dufour, R. J. 2002, *ApJ*, 565, 931
- Cannon, J. M., Walter, F., Skillman, E. D., & van Zee, L. 2005, *ApJL*, 621, L21
- Cormier, D., Leboutteiller, V., Madden, S. C., et al. 2012, *A&A*, 548, A20
- de Bennassuti, M., Schneider, R., Valiante, R., & Salvadori, S. 2014, *MNRAS*, 445, 3039
- Draine, B. T., et al. 2007, *ApJ*, 663, 866
- Draine, B. T., & Li, A. 2007, *ApJ*, 657, 810
- Dwek, E. 1998, *ApJ*, 501, 643
- Ekta, B., Pustilnik, S. A., & Chengalur, J. N. 2009, *MNRAS*, 397, 963
- Fisher, D. B., Bolatto, A. D., Herrera-Camus, R., et al. 2014, *Nature*, 505, 186
- Fumagalli, M., Krumholz, M. R., & Hunt, L. K. 2010, *ApJ*, 722, 919
- Galametz, M., Madden, S. C., Galliano, F., et al. 2011, *A&A*, 532, A56
- Giammanco, C., Beckman, J. E., Zurita, A., & Relaño, M. 2004, *A&A*, 424, 877
- Gnedin, N. Y., Tassis, K., & Kravtsov, A. V. 2009, *ApJ*, 697, 55
- Granato, G. L., Lacey, C. G., Silva, L., et al. 2000, *ApJ*, 542, 710
- Hirashita, H. 2015, *MNRAS*, 447, 2937
- Hirashita, H., Ferrara, A., Dayal, P., & Ouchi, M. 2014, *MNRAS*, 443, 1704
- Hirashita, H., & Voshchinnikov, N. V. 2014, *MNRAS*, 437, 1636
- Houck, J. R., Charmandaris, V., Brandl, B. R., et al. 2004, *ApJS*, 154, 211
- Hunt, L., Bianchi, S., & Maiolino, R. 2005a, *A&A*, 434, 849
- Hunt, L. K., Dyer, K. K., & Thuan, T. X. 2005b, *A&A*, 436, 837
- Hunt, L. K., Dyer, K. K., Thuan, T. X., & Ulvestad, J. S. 2004, *ApJ*, 606, 853
- Hunt, L. K., & Hirashita, H. 2009, *A&A*, 507, 1327
- Hunt, L., Magrini, L., Galli, D., et al. 2012, *MNRAS*, 427, 906
- Hunt, L. K., Testi, L., Casasola, V., et al. 2014, *A&A*, 561, AA49
- Hunt, L. K., Thuan, T. X., & Izotov, Y. I. 2003, *ApJ*, 588, 281
- Hunt, L. K., Vanzi, L., & Thuan, T. X. 2001, *A&A*, 377, 66
- Issa, M. R., MacLaren, I., & Wolfendale, A. W. 1990, *A&A*, 236, 237
- Ivezic, Z., & Elitzur, M. 1997, *MNRAS*, 287, 799
- Izotov, Y. I., Chaffee, F. H., Foltz, C. B., et al. 1999, *ApJ*, 527, 757
- Izotov, Y. I., Guseva, N. G., Fricke, K. J., Krügel, E., & Henkel, C. 2014, *A&A*, 570, A97
- Johnson, K. E., Hunt, L. K., & Reines, A. E. 2009, *AJ*, 137, 3788
- Jones, A. P., Fanciullo L., Köhler M., Verstraete L., Guillet V., Bocchio M., Ysard N. 2013, *A&A*, 558, 62
- Jones, A. P., & Nuth, J. A. 2011, *A&A*, 530, AA44
- Kassim, N. E., Weiler, K. W., Erickson, W. C., & Wilson, T. L. 1989, *ApJ*, 338, 152
- Kennicutt, R. C., Jr. 1984, *ApJ*, 287, 116
- Krumholz, M. R., McKee, C. F., & Tumlinson, J. 2009a, *ApJ*, 693, 216
- Krumholz, M. R., McKee, C. F., & Tumlinson, J. 2009b, *ApJ*, 699, 850
- Krumholz, M. R., Dekel, A., & McKee, C. F. 2012, *ApJ*, 745, 69
- Leboutteiller, V., Cormier, D., Madden, S. C., et al. 2012, *A&A*, 548, A91
- Lelli, F., Verheijen, M., Fraternali, F., & Sancisi, R. 2012, *A&A*, 537, AA72
- Leroy, A. K., Bolatto, A., Gordon, K., et al. 2011, *ApJ*, 737, 12
- Madden, S. C., Rémy-Ruyer, A., Galametz, M., et al. 2013, *PASP*, 125, 600
- Magrini, L., Bianchi, S., Corbelli, E., et al. 2011, *A&A*, 535, AA13
- Martin, C. L. 1997, *ApJ*, 491, 561
- Muñoz-Mateos, J. C., Gil de Paz, A., Boissier, S., et al. 2009, *ApJ*, 701, 1965
- Ota, K., Walter, F., Ohta, K., et al. 2014, *ApJ*, 792, 34
- Peeples, M. S., Werk, J. K., Tumlinson, J., et al. 2014, *ApJ*, 786, 54
- Plante, S., & Sauvage, M. 2002, *AJ*, 124, 1995
- Pustilnik, S. A., Brinks, E., Thuan, T. X., Lipovetsky, V. A., & Izotov, Y. I. 2001, *AJ*, 121, 1413
- Raiteri, C. M., Villata, M., & Navarro, J. F. 1996, *A&A*, 315, 105
- Recchi, S., Matteucci, F., D'Ercole, A., & Tosi, M. 2002, *A&A*, 384, 799
- Reines, A. E., Johnson, K. E., & Hunt, L. K. 2008, *AJ*, 136, 1415
- Reines, A. E., Nidever, D. L., Whelan, D. G., & Johnson, K. E. 2010, *ApJ*, 708, 26
- Rémy-Ruyer, A., Madden, S. C., Galliano, F., et al. 2013, *A&A*, 557, A95
- Rémy-Ruyer, A., Madden, S. C., Galliano, F., et al. 2014, *A&A*, 563, AA31
- Salvadori, S., Schneider, R., & Ferrara, A. 2007, *MNRAS*, 381, 647
- Schaerer, D., Boone, F., Zamojski, M., et al. 2015, *A&A*, 574, AA19
- Schmidt, K.-H., & Boller, T. 1993, *Astronomische Nachrichten*, 314, 361
- Skibba, R. A., Engelbracht, C. W., Dale, D., et al. 2011, *ApJ*, 738, 89
- Smith, B. J., & Hancock, M. 2009, *AJ*, 138, 130
- Thuan, T. X., & Izotov, Y. I. 1997, *ApJ*, 489, 623
- Thuan, T. X., Izotov, Y. I., & Lipovetsky, V. A. 1997, *ApJ*, 477, 661
- Thuan, T. X., Sauvage, M., & Madden, S. 1999, *ApJ*, 516, 783
- Valiante, R., Schneider, R., Bianchi, S., & Andersen, A. C. 2009, *MNRAS*, 397, 1661
- Valiante, R., Schneider, R., Salvadori, S., & Bianchi, S. 2011, *MNRAS*, 416, 1916
- Valiante, R., Schneider, R., Maiolino, R., Salvadori, S., & Bianchi, S. 2012, *MNRAS*, 427, L60
- Valiante, R., Schneider, R., Salvadori, S., & Gallerani, S. 2014, *MNRAS*, 444, 2442
- van den Hoek, L. B., & Groenewegen, M. A. T. 1997, *A&AS*, 123, 305
- van Zee, L., Westpfahl, D., Haynes, M. P., & Salzer, J. J. 1998, *AJ*, 115, 1000
- Vanzi, L., Hunt, L. K., Thuan, T. X., & Izotov, Y. I. 2000, *A&A*, 363, 493
- Watson, D., Christensen, L., Kraiberg Knudsen, K., et al. 2015, arXiv:1503.00002, *Nature*, in press
- Wolfire, M. G., McKee, C. F., Hollenbach, D., & Tielens, A. G. G. M. 2003, *ApJ*, 587, 278
- Woosley, S. E., & Weaver, T. A. 1995, *ApJS*, 101, 181
- Zaritsky, D., Kennicutt, R. C., Jr., & Huchra, J. P. 1994, *ApJ*, 420, 87

Zhukovska, S., Gail, H.-P., & Tieloff, M. 2008, A&A, 479, 453